A flexible, plane-wave-based formulation of continuum elasticity and multiband $\mathbf{k} \cdot \mathbf{p}$ models

Oliver Marquardt, Stefan Schulz,
Eoin P. O'Reilly
Tyndall National Institute
Lee Maltings, Cork, Ireland
Email: oliver.marquardt@tyndall.ie

Christoph Freysoldt, Sixten Boeck, Tilmann Hickel,
Jörg Neugebauer
Max-Planck-Institut für Eisenforschung GmbH
Max-Planck-Straße 1, 40237
Düsseldorf, Germany

***Abstract*—We present a highly flexible, plane-wave based formulation of continuum elasticity and multiband $\mathbf{k} \cdot \mathbf{p}$-formalism to study the elastic and electronic properties of semiconductor nanostructures. This approach has been implemented in the framework of the density functional theory (DFT) software library S/Phi/nX [1] and allows the investigation of arbitrary-shaped nanostructures such as quantum wells, wires and dots consisting of various materials. Moreover, our approach grants the flexibility to employ user-generated $\mathbf{k} \cdot \mathbf{p}$ Hamiltonians suited to the requirements of the study regarding accuracy and computational costs.**

I. Introduction

The $\mathbf{k} \cdot \mathbf{p}$ formalism has already been successfully applied to a wide range of semiconductor nanostructures such as quantum wells, wires and dots and is, due to its good accuracy and its small computational costs, a common tool to investigate nanostructured systems [2], [3]. Elastic properties that modify the bulk electronic properties of the system can be calculated using second-order continuum elasticity theory and are incorporated in common $\mathbf{k} \cdot \mathbf{p}$ models [4]. The 8-band $\mathbf{k} \cdot \mathbf{p}$ formalism is nowadays widely applied for nanostructured systems and was found to provide a better qualitative and quantitative description than the effective-mass approach. We have recently introduced a plane-wave based formulation of both the second-order continuum elasticity theory and an 8-band $\mathbf{k} \cdot \mathbf{p}$ model that conserves the spatially resolved properties of the provided nanostructure geometry. This formulation together with the existing, highly optimized minimization schemes of the plane-wave program package S/Phi/nX yield an excellent efficiency of the code [5].

However, the widely-used 8-band $\mathbf{k} \cdot \mathbf{p}$ approach used to describe the electrooptical properties of zincblende (ZB) semiconductor nanostructures suffers from a simplified and thus inaccurate description of the underlying crystal structure, as it neglects the bulk-inversion asymmetry (BIA) [6]. For the example of a square-based, pyramidal quantum dot (QD) in a ZB lattice, an atomistic description reduces the C_{4v}-symmetry of the pyramidal dot to a C_{2v}-symmetry as a result of dot geometry and underlying crystal lattice, since the system lacks the inversion symmetry [7]. This inaccuracy of the 8-band $\mathbf{k} \cdot \mathbf{p}$ model introduces artificial degeneracies, e.g., of the p-like first excited electron states in a square-based ZB QD [8], also shown in a comparison with atomistic tight-binding calculations in Ref. [9].

The correct symmetry properties of the underlying crystal lattice can be simulated by taking a higher number of directly considered bands into account [10], [11]. Additionally, a correct description of the whole Brillouin zone within a $\mathbf{k} \cdot \mathbf{p}$ formulation allows to apply this continuum approach to study indirect band gap semiconductor nanostructures, e.g., Si or Ge-based nanostructures. The higher accuracy of a more sophisticated model, of course, comes with the cost of a higher computational effort.

We have therefore generalized our approach from Ref. [5] to arbitrary-size $\mathbf{k} \cdot \mathbf{p}$ Hamiltonians that can be flexibly defined in a separate input file, without compromising computational efficiency. Each matrix element is constructed from momentum operators, strain fields, potentials, and material-dependent parameters, and meaningful combinations thereof. Material parameters are interpolated from the pure materials to the local alloy composition. This gives the freedom to choose a model that provides the best suited ratio of accuracy and efficiency for a given problem. As an example, we will present 8-band model calculations including strain and piezoelectric potentials performed for [111]-oriented InGaAs/GaAs QDs. Additionally, we compare 2+6-, 8-, and 14-band $\mathbf{k} \cdot \mathbf{p}$ bandstructures in InAs to evaluate the description of the BIA in $\mathbf{k} \cdot \mathbf{p}$ models of different levels of sophistication.

II. Electronic properties of III-V semiconductor nanostructures

A. [111]-oriented InGaAs/GaAs quantum dots

We have employed our formalism using the 8-band $\mathbf{k} \cdot \mathbf{p}$ Hamiltonian introduced by Bahder [4] to study the electronic properties of $In_xGa_{1-x}As$/GaAs QDs grown along the [111]-direction, as experimentally realized in Refs. [12], [13]. Such QDs allow, in principle, the generation of entangled photons. In fact, a strongly reduced fine structure splitting (FSS) has been observed in such QDs, recently [14]. We take the existence of degenerate excited electron states as an indicator for the symmetry of the system, i.e., to evaluate if the symmetry of the proposed QD is high enough to allow for the generation of entangled photons.

Figure 1 shows the polarization potential for an

978-1-61284-878-5/11/$26.00 ©2011 IEEE

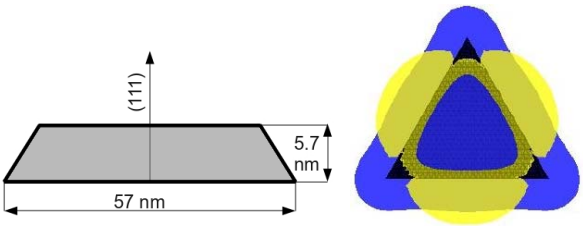

Fig. 1. Left: Side-view of the model QD geometry. Right: Polarization potential in a truncated pyramidal, [111]-grown $In_{0.35}Ga_{0.65}As$-QD, seen from the top. Blue (yellow) isosurfaces represent a polarization potential of -6 (8.8) mV. The dot is marked as a black lined triangle (Color online).

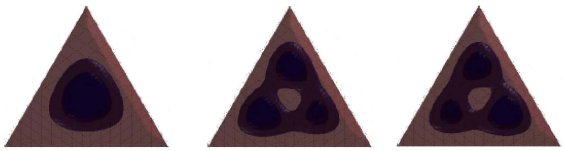

Fig. 2. Electron ground state (left) and first two excited electron states charge densities (middle and right) in the above QD. The corresponding eigenenergies are: 5.023 eV, 5.133 eV and 5.133 eV (Color online).

$In_{0.35}Ga_{0.65}As$ QD with a base length of 57 nm and a height of 5.7 nm in the shape of a triangular-based, truncated pyramid. The potential was computed from the strains that were derived from second-order continuum elasticity theory (for details, see Ref. [5]). Both strain and polarization potential enter the calculation of the QD single particle states and energies. As the underlying crystal lattice along the [111] direction as well as the QD geometry exhibit a C_{3v}-symmetry, an 8-band $\mathbf{k}\cdot\mathbf{p}$ model is suited to provide an accurate description of the electronic properties. In particular, the FSS is expected to be correctly described. Additionally, strain and polarization potentials do not reduce this symmetry, as they do commonly in [001]-grown C_{4v}-symmetric QDs. In fact, the calculation of the first three electron states in this QD yields a degenerate pair of excited states, suggesting a symmetry high enough to expect zero FSS. As realistic [111]-grown, site-controlled QDs show a much smaller aspect ratio with base lengths of approx. 80 nm and heights of 1.5 to 2 nm [15], a rotated $\mathbf{k}\cdot\mathbf{p}$-model that suits the [111]-growth direction, allows a much higher efficiency of the calculations, since the grid discretization can be chosen differently along the growth and the in-plane directions. These modifications can be easily incorporated in our model and are discussed in separate publications [16], [17].

B. Multiband $\mathbf{k}\cdot\mathbf{p}$ studies of InAs and GaAs

The widely used 8-band $\mathbf{k}\cdot\mathbf{p}$ Hamiltonian for the ZB structure is known to neglect the BIA in ZB III-V-semiconductors [6]. This simplification induces artificial degeneracies of electronic states, e.g., of the first two p-like electron states in QD geometries exhibiting a C_{4v}-symmetry. As a splitting between these two states is solely an effect of correctly describing the BIA in such a QD, it can be seen in atomistic calculations that include the BIA even if the influence of strain and polarization potentials are neglected [9], [8]. However, a higher number of explicitly treated bands in

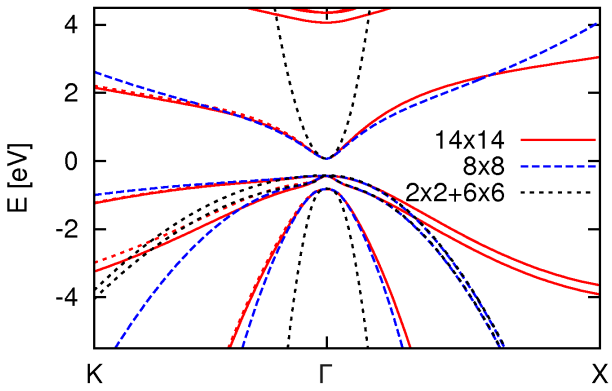

Fig. 3. InAs bulk band structure obtained from 2+6-band (black dotted), 8-band (blue dashed) and 14-band (red solid and dashed) $\mathbf{k}\cdot\mathbf{p}$-models (Color online).

a $\mathbf{k}\cdot\mathbf{p}$ model can help to correct this simplification in cases where a more sophisticated description is required [6]. As a first step to the investigation of QDs, we have thus employed the 14-band $\mathbf{k}\cdot\mathbf{p}$-Hamiltonian suggested in Ref. [18] for the bulk electronic properties of InAs. The resulting band structure is shown in Fig. 3. In fact, it can be seen that a splitting of valence bands obtained from the 14-band model is observed towards the K-point, which is not found in the 8-band model (solid and dashed red lines). Correspondingly, a splitting of p-like states in pyramidal InAs QDs is expected already without the influence of strain and polarization and will be discussed in a separate publication [19].

REFERENCES

[1] S. Boeck, C. Freysoldt, A. Dick, L. Ismer and J. Neugebauer, Computer Phys. Commun. **182**, 543, 2011.
[2] A. Schliwa, M. Winkelnkemper and D. Bimberg, Phys. Rev. B **76**, 205324, 2007.
[3] O. Marquardt, T. Hickel and J. Neugebauer, J. Appl. Phys. **106**, 083707, 2009.
[4] T. Bahder, Phys. Rev. B **41**, 11992, 1990.
[5] O. Marquardt, S. Boeck, C. Freysoldt, T. Hickel and J. Neugebauer, Computer Phys. Commun. **181**, 765, 2010.
[6] J.M. Jancu, R. Scholz, E.A. de Andrada e Silva and G.C. La Rocca, Phys. Rev. B **72**, 193201, 2005.
[7] N. Baer, S. Schulz, P. Gartner, S. Schumacher, G. Czycholl, and F. Jahnke, Phys. Rev. B **76**, 075310 (2007)
[8] G. Bester and A. Zunger, Phys. Rev. B **71**, 045318, 2005.
[9] O. Marquardt, D. Mourad, S. Schulz, T. Hickel, G. Czycholl and J. Neugebauer, Phys. Rev. B **78**, 235302, 2008.
[10] U. Rössler, Solid State Commun. **49**, 943, 1984.
[11] M. Cardona, N.E. Christensen and G. Fasol, Phys. Rev. B **38**, 1806, 1988.
[12] E. Pelucchi, S. Watanabe, K. Leifer, Q. Zhu, B. Dwir, P. De Los Rios and E. Kapon, Nano Lett. **7**, 1282, 2007.
[13] Q. Zhu, K.F. Karlsson, E. Pelucchi and E. Kapon, Nano Lett. **7**, 2227, 2007.
[14] E. Stock, T. Warming, I. Ostapenko, S. Rodt, A. Schliwa, J.A. Toffflinger, A. Lochmann, A.I. Toropov, S.A. Moshchenko, D.V. Dmitriev, V.A. Haisler and D. Bimberg, Appl. Phys. Lett. **96**, 93112, 2010.
[15] S.B. Healy, R.J. Young, L.O. Mereni, V. Dimastrodonato, E. Pelucchi and E.P. O'Reilly Physica E **42**, 2761, 2009.
[16] S. Schulz, M. Caro, E.P. O'Reilly and O. Marquardt, to be submitted.
[17] O. Marquardt, E.P. O'Reilly and S. Schulz, in preparation.
[18] P. Pfeffer and W. Zawadzki, Phys. Rev. B **53**, 12813, 1996.
[19] O. Marquardt and E.P. O'Reilly, in preparation.